Penning Ionization Electron Spectroscopic and Ab Initio Study of the Interaction and Ionization of HNCO and HNCS with He*(2^3S) Metastable and Li(2^2S) Ground State Atoms

Tibor Pasinszki,*,† Naoki Kishimoto, and Koichi Ohno*,‡

Department of Chemistry, Graduate School of Science, Tohoku University, Aramaki, Aoba-ku, Sendai, 980-8578, Japan

Received: June 28, 1999; In Final Form: September 20, 1999

The electronic structure and ionization of HNCO and HNCS were studied in the gas phase by two-dimensional Penning and He I photoelectron spectroscopies. From experimental data the anisotropy of the interaction between molecules (M) and He*(2^3S) atoms were deduced. The interaction potential for the similarly interacting M-Li(2^2S) system was obtained from ab initio calculations at the CCSD(fc)/6-311++G** level. Experimental and calculated results showed that the interaction potential was attractive in the π orbital region of molecules and in the terminal oxygen lone electron pair region of HNCO, and the interaction was repulsive around the hydrogen atom. From the anomalies in the experimental results and from theoretical calculations, the breakdown of the MO picture for ionization of HNCS in the 15−20 eV region was concluded. The spectroscopic investigations predicted the existence of thermodynamically stable MLi radicals, and the structure and stability of HNCOLi and HNCSLi were calculated at the QCISD(fc)/6-311++G** level.

I. Introduction

Due to their varied structure, stability, and reactivity, pseudohalides continuously attract attention from researchers in various field of chemistry. They are unsaturated and usually exhibit large amplitude deformations, thus the description of their physical and chemical behavior requires the application of the most sophisticated theoretical methods. In many cases they serve as an example for the downfall of generally accepted and well performing theoretical methods. We have recently started to investigate the pseudohalide acids HCNO and HNNN[1] by Penning ionization electron spectroscopy (PIES) and ab initio calculations to obtain information about their electronic structure and their interaction with He*(2^3S) and Li(2^2S) atoms. These investigations showed that there was an unusually strong attractive interaction between molecules and He*(2^3S) metastable atoms, as well as that HCNO and HNNN formed stable four-membered π complexes with lithium atom. To further investigate these novel chemical behaviors on similar systems initiated the present work on HNCO and HNCS. This work, however, proved again that pseudohalides deserve special attention: we observed experimentally, and show below, the breakdown of the molecular orbital picture in the Penning ionization process and discuss its consequences.

In Penning ionization electron spectroscopy, molecules (M) are collided with metastable rare gas atoms, He*(2^3S) in this work, having higher excitation energy than the ionization potential (IP) of molecules, and the kinetic energy (E_{ek}) of the ejected electrons (e^-) is analyzed

$$M + He^*(2^3S) \rightarrow M_i^+ + He + e^- \qquad (1)$$

The energy of the ejected electron depends on the potential energy difference between the incoming M + He*(2^3S) (called interaction potential) and outgoing M_i^+ + He systems at the geometry of ionization and provides information about the ionic state (M_i^+) formed, as well as the electronic structure of the molecule. Since the electron energy is determined by the incoming and outgoing potential, PIES does not necessary provide IPs, unlike, e.g., He I photoelectron spectroscopy (UPS), and thus there are small peak shifts if UPS and PIES spectra are compared to each other on an electron kinetic energy scale taking the energy of the photons and metastable atoms into account. The outgoing potential, in general, can be assumed as flat in the ionization region, thus information on the interaction potential can be obtained from the peak shifts (ΔE_i). In a simplified sense one can expect that ΔE_i is positive if the interaction is repulsive and negative if the interaction is attractive. In this latter case the peak shift is the measure of the well depth of the attractive interaction potential. Since in the outer valence molecular orbital (MO) region the ionization can usually be described as removing an electron from a MO, the peak shift reflects the interaction potential in the molecular region where the MO is localized.

The branching ratios in PIES spectra are determined by the ionization cross sections (σ): attractive interaction is expected to increase the ionization cross section by increasing the number of trajectories leading to ionization, and repulsive interaction to decrease the ionization cross section. It is clear, therefore, that if the interaction is attractive or repulsive, the ionization cross section depends on the metastable atom collision energy, and vice versa the collision energy dependence of the ionization cross section provides information about the interaction. Two-dimensional Penning ionization electron spectroscopy (2D-PIES) has been recently developed in our laboratory,[2] in which ionization cross sections are determined as a function of both electron kinetic energy and metastable atom collision energy. The method, thus ionic state and collision energy resolved, makes it possible to study the collision energy dependence of the total and partial ionization cross sections. One-dimensional

* Corresponding authors.
† Permanent address: Department of Inorganic Chemistry, Technical University, H-1521 Budapest, Hungary.
‡ E-mail: ohnok@qpcrkk.chem.tohoku.ac.jp.

10.1021/jp992174c CCC: $18.00
Published on Web 11/03/1999

cuts from the two-dimensional spectrum give the collision energy dependence of partial ionization cross sections (CEDPICS; ionic state is fixed) and collision-energy-resolved PIES (CERPIES; metastable atom kinetic energy is constant). Since, and if, an ionic state originates from removing an electron from a molecular orbital, the dependence of the partial ionization cross section reflects the interaction between molecule and metastable atom in the molecular region where the MO is localized.

As we can see from the discussion above, the molecular orbital model is essential for the discussion and description of the anisotropy of the interaction potential around molecules. Fortunately the molecular orbital picture for ionization is valid or a good approximation in the IP region below ca. 20 eV. We have successfully applied the CERPIES and the recently developed 2D-PIES techniques to study the interaction between He*(2^3S) and various organic molecules and interpreted the results in the frame of the molecular orbital picture.[3−14] It has been observed that the interaction is repulsive around saturated hydrocarbons, alkyl groups, or CH bonds,[3−8,11,13,14] but attractive around the π region of unsaturated hydrocarbons,[5,6] heterocycles,[8] and C═O double bonds.[6] Studies of alcohols,[7,13] aldehides,[6] ethers,[7,9] amines,[10] isocyanates,[11] nitriles,[3,10,14] and isonitriles,[3] have indicated that the interaction is attractive in the lone electron pair region of first-row nonmetal atoms (O, N, and C). According to the few studies on molecules containing heavier elements, which focus on organic chlorides and sulfur compounds, the interaction potential is attractive around the chlorine atom,[4,12] but in the case of the sulfur atom it is strongly dependent on the molecular environment: a very attractive potential was found in the sulfur lone pair region in alkyl thioethers and thioalcohols,[13] but no special character (only weakly attractive or weakly repulsive) was found in the sulfur lone pair region of methyl thiocyanate,[11] methyl isothiocyanate,[11] and thiophene.[8] On the basis of previous studies, it is clear that a chemical group shows characteristic interaction with He*(2^3S) and this interaction is strongly influenced by the molecular environment of the group; therefore, the study of the anisotropy of the interaction potential around various chemical groups and the effect of substituents on this is important for the understanding of collision mechanism and dynamics.

Penning spectroscopy is a powerful method to obtain direct information about the interaction potential between M and He*(2^3S). Since there is a similarity between M + He*(2^3S) and M + Li(2^2S) interaction potentials, it provides indirect information about this latter chemically important reaction, too, making a close link between PIES and lithium chemistry.[3] M + Li(2^2S) potential is the ground state potential of the M-Li system, thus a large, negative peak shift (deep well on the potential surface) in PIES indirectly indicates the existence of thermodynamically stable M-Li radicals, and if there is no large geometry relaxation of M in the MLi complex and the corresponding MO is localized, the peak shift is a good estimation of the bonding energy of the complex. On the basis of PIES investigations, we predicted, e.g., the existence of CH_3-CNLi[3] and this radical was identified recently in our laboratory in the gas phase by laser evaporation and subsequent reaction of lithium metal with CH_3CN vapors.[15]

In this paper we present a combined experimental (UPS, PIES) and theoretical study of the structure of HNCO and HNCS, and the first study of their interaction with He*(2^3S) and Li atoms using 2D-PIES and ab initio calculations. Relevant to this work are the earlier He I photoelectron spectroscopic investigations[16,17] and our previous CERPIES study on the methyl-substituted derivatives, CH_3NCO and CH_3NCS.[11] Of particular interest are the electronic structure of molecules, the anisotropy of the interaction between molecules and He*(2^3S) or Li(2^2S) atoms, as well as the possible existence, stability, and structure of M-Li inorganic radicals.

SCHEME 1

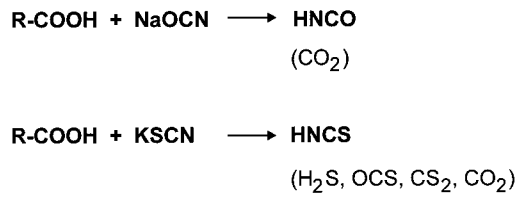

II. Experimental Section

HNCO and HNCS (HNCX) are weak acids and thus they can be liberated from their alkali salts with a stronger acid, e.g., with stearic acid (R−COOH, where R═$CH_3(CH_2)_{16}$−).[18] We have recently generated the similarly weak acid HNNN in an essentially clean route from its sodium salt by reacting it with molten stearic acid in high yield,[1] thus this route seemed to be promising and simple for HNCX as well. The applied procedure is briefly described below (see Scheme 1; volatile side products of the reaction are also shown). NaOCN, KSCN, and stearic acid were commercial products (Nacalai Tesque). NaOCN and stearic acid were used without purification. KSCN was dried in an oven at 60 °C for overnight and stored in a desiccator.

HNCO and HNCS were synthesized by solid−liquid reaction between sodium cyanide or potassium thiocyanate and molten stearic acid. NaNCX and solid stearic acid were mixed at room temperature, placed into a flask, which was connected directly to the spectrometer via a U-trap, and gradually warmed above the melting point of the acid to obtain a fast continuous bubbling of the gaseous products. The volatiles were condensed in the U-trap with liquid nitrogen, then the trap was separated and gradually warmed. Volatile side products were pumped off at low temperature, and then the temperature was raised to obtain sufficient vapor pressure for the spectroscopic investigations of HNCX. According to the UPS and PIES spectroscopic investigations and on the basis of repeated experiments, the HNCX samples were found to be pure. The very small features with negligible intensity in the low ionization energy region of PIES spectra can be derived from singlet metastable atom and He I photon impurities in the metastable atom beam. The weak feature between 7 and 8 eV electron energy in the UPS spectrum of HNCO may be attributed to He I(β) line in the photon source.

The instrument used in this work for recording the UPS, PIES, and 2D-PIES spectra was reported in previous papers.[2,4,5,19] UPS spectra were measured by utilizing the He I resonance line (21.22 eV) produced by a pure helium discharge. Metastable atoms for PIES were produced by a negative discharge nozzle source, and the He*(2^1S) component of the He*(2^1S,2^3S) beam was quenched by a water-cooled helium discharge lamp. The kinetic energies of electrons ejected by photo or Penning ionization were determined by a hemispherical electrostatic deflection type analyzer using an electron collection angle of 90° to the incident photon or He*(2^3S) beam axis. The energy resolution of the electron analyzer was 50 meV, estimated from the full width at half-maximum (fwhm) of the $Ar^+(^2P_{3/2})$ peak in the He I UPS spectrum. The transmission of the electron energy analyzer was determined by comparing our UPS data of O_2, CO, N_2, and some hydrocarbons with those of Gardner and Samson[20] and Kimura et al.[21]

In the collision-energy-resolved experiments, 2D-PIES, the metastable atom beam was pulsed by a pseudorandom chopper

and introduced into the reaction cell located 504 mm downstream from the chopper disk. As reference, the intensity of metastable atoms was determined by inserting a stainless steel plate into the reaction cell and measuring the intensity of secondary electrons emitted. The resolution of the electron energy analyzer was lowered to 250 meV (fwhm for He I UPS of Ar) in order to gain higher electron counting rates. Thus in these experiments the intensity of emitted electrons from sample molecules (I_e) or from a reference stainless steel plate (I_{He^*}) was measured as a function of electron kinetic energy (E_{ek}) and time (τ). Electron energies were scanned by 35 meV steps, and a dwell time for the time-dependent measurement was 3 μs. The 2D electron intensity spectra, $I(E_{ek},\tau)$, were then converted sequentially to $I(E_{ek},\tau_{TOF})$ and $I(E_{ek},\nu_{He^*})$ (where τ_{TOF} is the time-of-flight and ν_{He^*} is the velocity of the metastable atoms). The 2D Penning ionization cross section $\sigma(E_{ek},\nu_r)$ was obtained from $I(E_{ek},\nu_{He^*})$ using eqs 2 and 3, and finally $\sigma(E_{ek},\nu_r)$ was converted to the 2D-PIES, $\sigma(E_{ek},E_c)$, using eq 4

$$\sigma(E_{ek},\nu_r) = c[I_e(E_{ek},\nu_{He^*})/I_{He^*}(\nu_{He^*})](\nu_{He^*}/\nu_r) \quad (2)$$

$$\nu_r = [\nu_{He^*}2 + 3kT/M]^{1/2} \quad (3)$$

$$E_c = \mu\nu_r^2/2 \quad (4)$$

where c, ν_r, k, T, M, and μ are constants, the relative velocity of metastable atoms averaged over the velocity of the target molecule, the Boltzmann constant, the gas temperature (300 K), the mass of the target molecule, and the reduced mass of the system, respectively.

III. Calculations

To assist with experimental data, the interaction potential between target molecules (M) and metastable He*(2^3S) atoms was modeled by approximating the M-He*(2^3S) surfaces with those of M-Li(2^2S). Using this widely accepted approximation, based, e.g., on cross-scattering experiments indicating very similar shape for the velocity dependence of the total scattering cross section and for the location and depth of the well of the attractive interaction potential for He*(2^3S) and Li(2^2S) with various atomic and molecular targets,[22] all of the difficulties could be bypassed that would be associated with calculating the excited-state M-He* surfaces. Thus the M-Li(2^2S) interaction potentials, V*(R,θ) (where R is the distance from the center of mass (X) of the molecule, and θ is the Li−X−O or Li−X−S angle), were calculated by pulling the Li atom toward the center of mass of the molecules and keeping the molecular geometries fixed at the experimental values determined from microwave spectroscopic data;[23,24] this latter assumption meant that the geometry relaxation by the approach of the metastable atom was negligible in the ionization process. All calculations for the interaction potential were done at the CCSD(fc)/6-311++G** level of theory and the full counterpoise (CP) method[25] was used to correct for the basis-set superposition errors (BSSE).

The structure of HNCOLi and HNCSLi inorganic radicals was fully optimized at the QCISD(fc)/6-311++G** level of theory, taking advantage of the analytic first derivatives at this level in *Gaussian 94*, and then harmonic vibrational frequencies were calculated at the equilibrium geometries using numeric second derivatives to make sure they were real minima on the potential energy surface. In the case of HNCO, serious convergence problems in the post-HF iteration cycles appeared during the harmonic frequency calculations, and this could not be solved by changing the default step size; therefore, HNCO was recalculated at the B3LYP level, where we did not observe any convergence problem. Changing the step size in case of convergence problem was efficient for HNCS and in our previous work on HNNN as well.[1] Dipole moments and total atomic charges were calculated using the QCISD density and the natural population analysis. All calculations were performed with the *Gaussian 94* quantum chemistry package[26] implemented on Silicon Graphics Inc. Challenge/XL and Origin200 workstations.

The ionization potentials for HNCO and HNCS were calculated at the experimental geometries using the outer valence Green's function (OVGF) method[27] as incorporated in *Gaussian 94*.

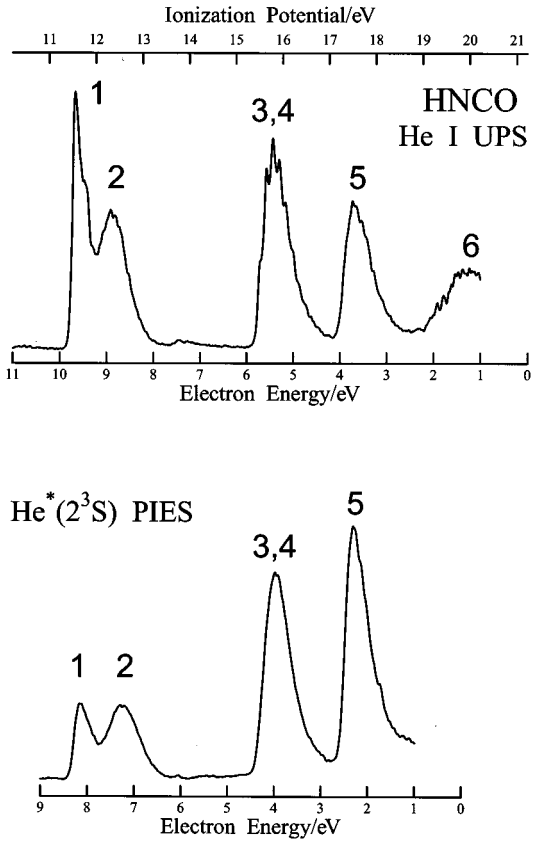

Figure 1. He I UPS and He*(2^3S) PIES spectrum of HNCO.

IV. Results

Figures 1 and 2 show the He I UPS and He*(2^3S) PIES spectra of HNCO and HNCS, respectively. The electron energy scales for PIES spectra are shifted relative to those of UPS by the difference in the excitation energies; 21.22 − 19.82 = 1.40 eV.

Figure 3 shows a representation of the 2D-PIES spectrum of HNCO and HNCS. The spectra in the figure are obtained from the experimental 2D-PIES spectra by cutting small collision energy regions.

Figures 4 and 5 show the log σ vs log E_c plots of CEDPICS for HNCO and HNCS, respectively. The CEDPICS are obtained from the 2D-PIES spectra by cutting an appropriate range of electron kinetic energy, E_e (typically the fwhm of the corresponding PIES band). The calculated electron density maps of molecular orbitals are also shown in the figures (the thick solid curve in the maps indicates the molecular surface, estimated from the van der Waals radii of atoms). Electron density contour

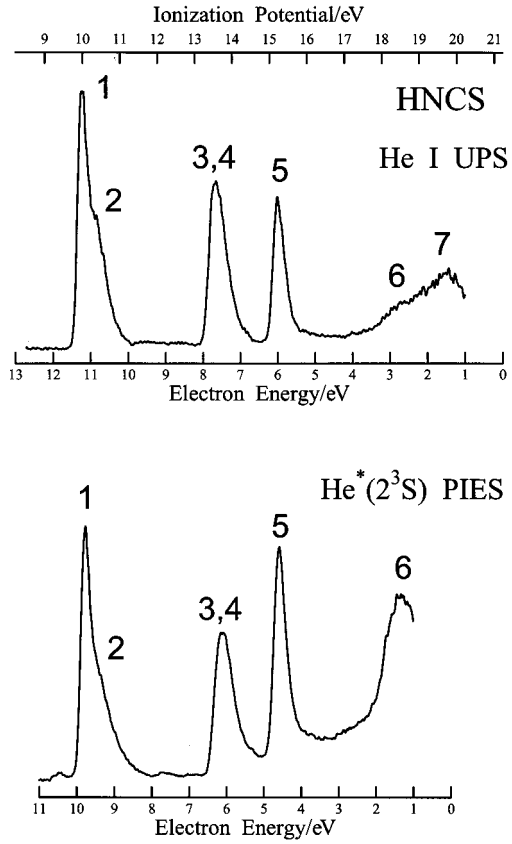

Figure 2. He I UPS and He*(2^3S) PIES spectrum of HNCS.

maps are shown in the symmetry plane of molecules for the a′ orbitals, and for the a″ orbitals one of those planes is selected, which are parallel to the symmetry plane of the molecules and lying just above the van der Waals radius of carbon.

Figures 6 and 7 show calculated potential energy curves between a ground-state Li atom and HNCO and HNCS, respectively. The potential energy is shown as a function of the distance between the Li atom and the center of mass of the molecule. Calculations are done at the CCSD/6-311++G** level of theory.

Figure 8 shows calculated geometry and natural atomic charges for HNCOLi-π and HNCSLi-π inorganic radicals. Calculations are done at the QCISD/6-311++G** level of theory.

Table 1 lists experimental and calculated ionization potentials (IPs), experimental peak energy shifts (ΔE), slope parameters (m), and the assignment of the spectra. Slope parameters are obtained from the log σ vs log E_c plots (for details of explaining the expected linear relationship between log σ and log E_c see, e.g., ref 3). Vertical IPs are determined from the He I UPS spectra. The peak energy shifts in PIES spectra are obtained as the difference between the peak position (E_{PIES}; electron energy scale) and the "nominal" value (E_0 = difference between the metastable excitation energy and target IP): $\Delta E = E_{PIES} - E_0$.

Table 2 lists calculated energies, dipole moments, rotational constants, harmonic vibrational frequencies, and infrared intensities for HNCOLi-π and HNCSLi-π. Calculations are done at the QCISD/6-311++G** level of theory, except the harmonic frequency calculation of HNCO-π, which is done at the B3LYP/6-311++G** level.

V. Discussion

A. Assignment of UPS and PIES Spectra. If the simple MO picture for ionization is valid (one electron ejection from a given MO, which produces the corresponding one hole ionic state), a band in UPS and PIES spectra can be assigned to ionization of a given orbital, and the peak shift and collision energy dependence of the partial ionization cross section reflect the interaction in the given MO region. A simple description of MOs of HNCO and HNCS, following Eland,[16] is as follows: if these molecules were linear, MOs of HNCO and HNCS (HNCX, X = O, S) would be of the same character as those of isoelectronic linear OCO and OCS, respectively, and the π orbitals would remain degenerate. In the real bent molecule, however, the degeneracy of both the bonding and nonbonding π orbitals is lifted to produce two pairs of orbitals of symmetry a″ and a′. In the simplest model, the orbital a′ derived from the nonbonding π orbital (π_{nb}) becomes a lone pair on the nitrogen atom and the a′ orbital derived from the bonding π orbital (π_b) becomes a pure C = X bond. The out-of-plane orbitals retain their original π character. The extent of the lone pair and double bond character, or their delocalization, however, depends on the deviation from linearity, and the delocalized and localized models may be regarded as the two most important mesomeric structures. For keeping the discussion simple, we use the π_{nb} and π_b symbols for HNCX in this paper. The UPS and PIES spectra of HNCO and HNCS are shown in Figures 1 and 2, respectively, with assignment, experimental IPs, and calculated IPs listed in Table 1. On the basis of previous

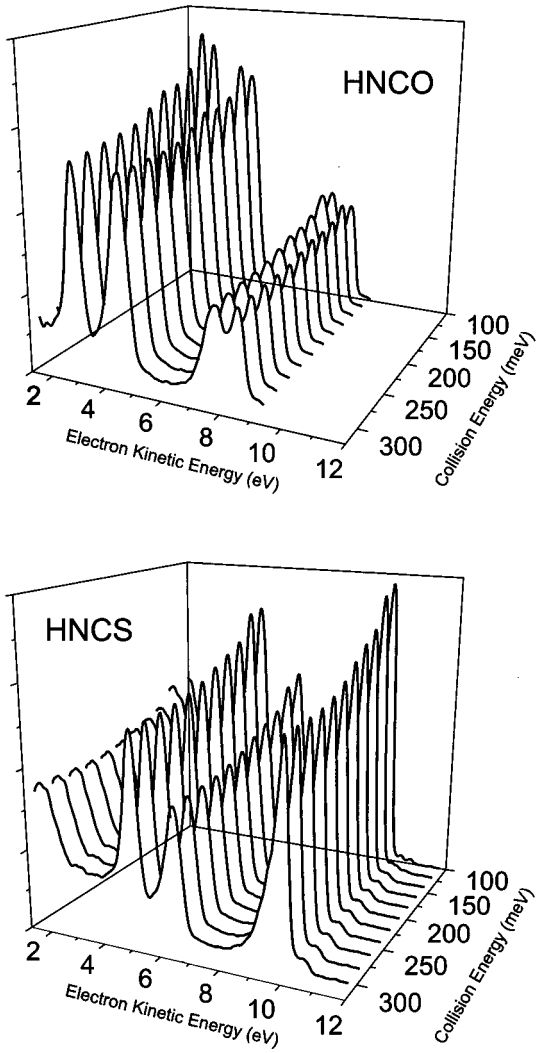

Figure 3. Representation of the 2D-PIES spectrum of HNCO (top) and HNCS (bottom). Curves (CERPIES spectra) are obtained from the 2D-PIES spectrum by cutting small kinetic energy regions.

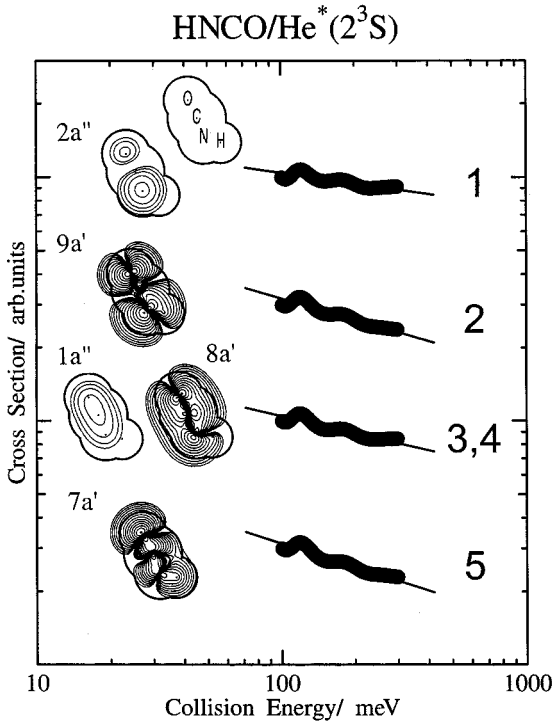

Figure 4. Collision energy dependence of partial ionization cross sections for HNCO with He*(2^3S).

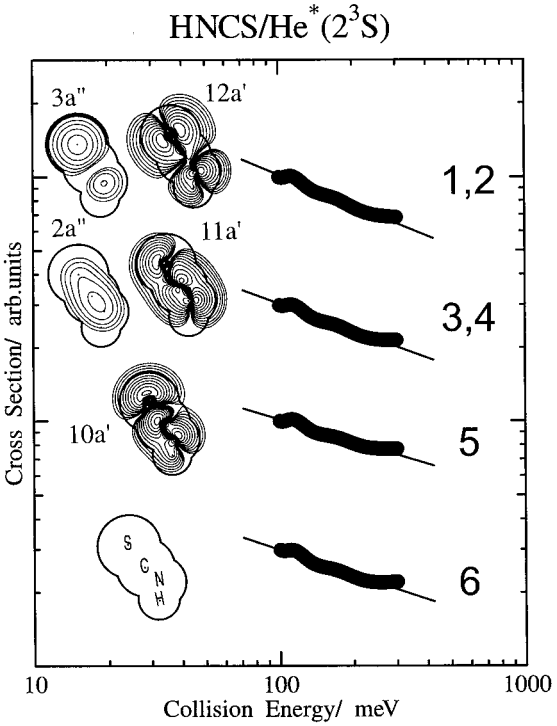

Figure 5. Collision-energy-dependence of partial ionization cross sections for HNCS with He*(2^3S).

and present He I UPS investigations, as well as calculations,[28,29] the assignment of spectra is relatively straightforward. Five bands are observed in the UPS spectrum of HNCO (see Figure 1). On the basis of the simple MO picture these bands can be assigned in the order of increasing IPs to ionization of $\pi_{nb}(a'')$, $\pi_{nb}(a')$, $\pi_b(a'') + \pi_b(a')$, oxygen terminal lone pair $n_O(a')$, and a $\sigma(a')$ MO, respectively. The last band at higher IPs is not observed in PIES due to the smaller excitation energy of metastable atoms than that of photons; therefore information

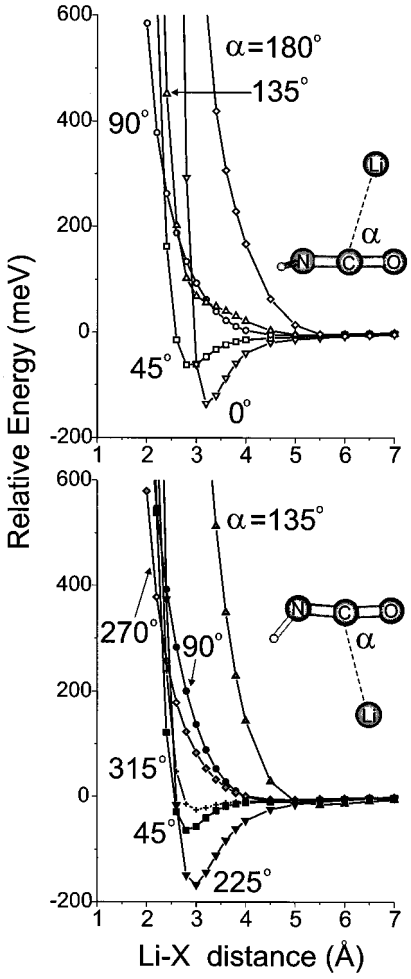

Figure 6. Calculated interaction potential curves between HNCO and Li(2^2S) as functions of distance between the Li atom and the center of mass of molecule (top, Li-X−O plane is perpendicular to the symmetry plane of the molecule; bottom, Li atom is in the symmetry plane of the molecule). Li-X−O angle is indicated for each curve.

about the interaction potential may be obtained in the $\pi_{nb}(a'')$, $\pi_{nb}(a')$, and $n_O(a')$ orbital region separately, as well as an average character of the interaction in the $\pi_b(a'') + \pi_b(a')$ orbital region due to the complete overlapping of the corresponding bands. The frame of HNCS is closer to linearity than that of HNCO, thus the splitting of $\pi(a'')$ and $\pi(a')$ MOs of HNCS is smaller than that of HNCO, and as a consequence the $\pi(a'')$ and $\pi(a')$ bands in UPS and PIES spectrum (Figure 2) strongly overlap. Three well separated bands are observed in the 9−17 eV IP region, and only a shoulder on the first band indicates the splitting of $\pi_{nb}(a'')$ and $\pi_{nb}(a')$ MOs. On the basis of simple MO picture, in agreement with the earlier assignment of this IP region,[16] the three bands can be assigned to ionization from $\pi_{nb}(a'') + \pi_{nb}(a')$, $\pi_b(a'') + \pi_b(a')$, and $n_S(a')$ MOs, respectively, in the order of increasing IPs, which would make it possible to study the anisotropy of the interaction potential in the π_{nb}, π_b, and n_S MO region. There are at least two additional bands in the high IP region of the UPS spectrum (Figure 2). Since on the basis of calculations and simple electronic structure considerations only one band is expected in this region from simple one hole ionization (from $9a'(\sigma)$ MO), one of these bands must be assigned to $9a'(\sigma)$ MO and the others to shake-up bands (simultaneous ionization-excitation two-electron process; two-hole-one-particle (2h1p) state). The assignment, however, is not clear. The two strongest (with largest pole strength) are marked with numbers of 6 and 7 in Figure 2 and Table 1. Previous

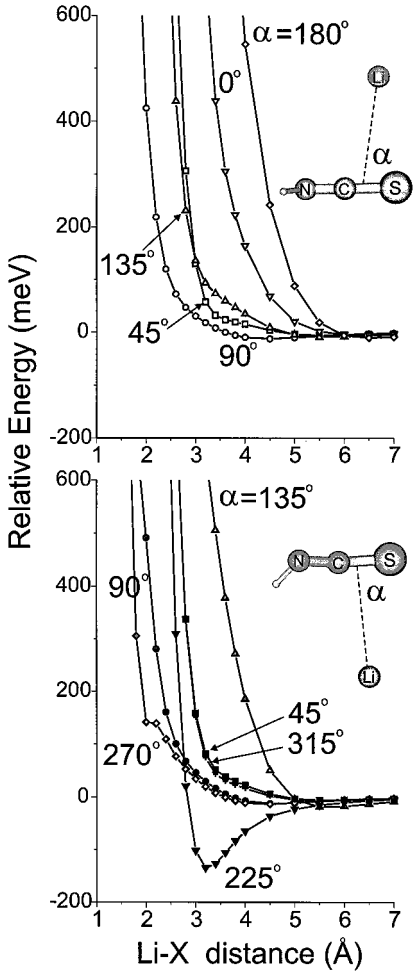

Figure 7. Calculated interaction potential curves between HNCS and Li(2^2S) as functions of distance between the Li atom and the center of mass of the molecule (top, Li-X−S plane is perpendicular to the symmetry plane of the molecule; bottom, Li atom is in the symmetry plane of the molecule). Li-X−S angle is indicated for each curve.

calculation using the so-called extended 2ph-TDA Green's function method (see Table 1),[29] which systematically takes into account the 2h1p states and the coupling of the 2h1p excitations and the simple hole states, predicts the appearance of numerous shake-up bands in the 15−20 eV region. There are very small features in UPS spectrum in 16−18 eV IP region, which may originate from shake-up processes. Shake-up bands usually have higher relative intensity in PIES than in UPS, and PIES spectra clearly show the appearance of these bands in the 16−18 eV IP region.

As Figures 1 and 2 show, relative band intensities in PIES and UPS spectra are very different compared to each other, reflecting differences in their ionization mechanism. In the Penning ionization process, an electron in a MO of target molecule is transferred into the inner half-filled 1s orbital of He*(2^3S), and the excited 2s electron of He*(2^3S) is ejected.[30] The probability of the electron transfer depends on the overlap between the MO of molecule and 1s orbital of He*(2^3S); therefore, the relative band intensity in PIES reflects the exterior electron distribution of the MO exposed to the outside of the boundary surface of collision.[31,32] In the PIES spectrum of HNCO, the intensity of the fifth band corresponding to ionization of terminal oxygen lone electron pair $n_O(a')$ is strongly enhanced. Similar strong relative intensity of a terminal lone electron pair PIES band has been observed previously for nitriles, isonitriles, and thiocyanates,[3,11] thus the large electron

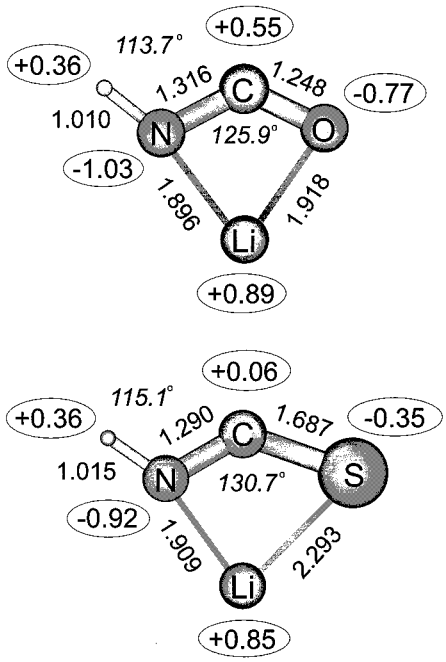

Figure 8. Calculated structure and total atomic charges of HNCOLi and HNCSLi radicals (distances in angstrom).

density exposed to the outside of the boundary surface of collision at the terminal lone pair seems to be one of the characteristics of pseudohalide electronic structure. This electronic structure may explain the known ability of pseudohalides to form various complexes via the terminal lone pair dative bond. The intensity of $\pi_{nb}(a')$ band (band 2 in the PIES spectrum) is about two times stronger than $\pi_{nb}(a'')$ band (band 1). Because $\pi_{nb}(a')$ MO has a large nitrogen imine type lone pair character, this lone pair is exposed much stronger to the outside of the boundary surface of collision than $\pi_{nb}(a'')$ MO. It is interesting to find that the intensity of $\pi_b(a' + a'')$ bands (3,4) is stronger than that of $\pi_{nb}(a' + a'')$ bands. The nonbonding π_{nb} MOs has a nodal surface on the central carbon atom and thus they are localized on the nitrogen and oxygen atoms. Bonding π_b MOs has a large electron density on the central carbon atom. The intensity of PIES bands shows that in the π MO region larger electron density is exposed to the outside of the boundary surface of collision at the central carbon atom than at the two ends of the NCO frame. The situation is just the opposite in PIES spectrum of HNCS. Since nonbonding π_{nb} MOs have larger electron density on the heavy sulfur atom than bonding π_b MOs, they are exposed to the outside of the boundary surface of collision to a larger extent than π_b MOs and consequently have larger intensity in PIES spectrum. The terminal sulfur lone pair band $n_S(a')$ (band 5) has again a strong relative intensity in the PIES spectrum, especially comparing it to $\pi_b(a' + a'')$ bands. It must be noted, however, that due to the breakdown of the molecular orbital picture for ionization of HNCS in the 15−20 eV region the $n_S(a')$ and $\pi_b(a')$ bands may "borrow" some intensity from each other (see below).

B. 2D-PIES and Interaction Potential. Representations of the 2D-PIES spectra and CEDPICS spectra of HNCO and HNCS are shown in Figures 3 and 4 and 5, respectively, and calculated Li-M interaction potential curves are shown in Figures 6 and 7. Experimental data clearly show that the interaction between HNCO and He*(2^3S) is attractive in the π and terminal oxygen lone pair region: all peak shifts and slope parameters are negative (see Table 1). This is in agreement with calculated Li-M potential curves, which show fine details of the anisotropy

TABLE 1: Band Assignments, Ionization Potentials (IP/eV), Peak Energy Shifts (Δ*E*/MeV), and Slope Parameters (*m*) for HNCO and HNCS

molecule	band	IP/eV exp	IP/eV calcd[a]	orbital character	Δ*E*/meV (±20 meV)	*m* (±0.03)
HNCO	1	11.55	11.38 (0.91)	2a″(π_{nb})	−100	−0.15
	2	12.31	12.11 (0.91)	9a′(π_{nb})	−240	−0.29
	3	15.79	16.03 (0.88)	8a′(π_b)	−40	−0.23
	4		16.17 (0.87)	1a″(π_b)		
	5	17.49	17.98 (0.90)	7a′(n_O)	−20	−0.32
	6	20.0	20.54 (0.90)	6a′(σ)		
HNCS	1	9.97	9.50 (0.91)[b]	3a″(π_{nb})	−100	−0.42
	2	(10.4)	9.91 (0.91)[b]	12a′(π_{nb})		
	3	13.58	13.72 (0.085; 0.58)[c]	11a′(π_b)	−160	−0.37
	4		13.93 (0.55)	2a″(π_b)		
	5	15.21	15.08 (0.67; 0.16)[c]	10a′(n_S)	−40	−0.30
			15.12 (0.16)[d]			
			15.87 (0.041; 0.048)[c]			
	6	18.49	19.84 (0.12)[d]		0	−0.34
			20.23 (0.079; 0.036)[e]			
	7	19.70	20.27 (0.16)	9a′(?)		
			20.59 (0.34; 0.02; 0.03)[f]			

[a] OVGF calculations (this work) for HNCO and extended 2ph-TDA Green's function calculations for HNCS from ref 28 (pole strength in parentheses). [b] OVGF calculations (this work). [c] The Green's function is nondiagonal in the 10a′ and 11a′ orbital indices; the pole strengths given in parentheses refer to these two ionization processes in the given order.[28] [d] Calculated satellite band of the 2a″ ionization. [e] Nondiagonality of the Green's function in the 9a′ and 10a′ orbital indices. [f] Nondiagonality of the Green's function in the 9a′, 10a′, and 11a′ orbital indices.

TABLE 2: Calculated Rotational Constants (GHz), Dipole Moments (Debye), Total Energies (au), Bonding Energies (kJ/mol), Harmonic Vibrational Frequencies (cm^{-1}), and IR Intensities (km/mole) of HNCOLi and HNCSLi[a]

HNCOLi-π		HNCSLi-π	
A[b] 24.4826		*A*[b] 22.5947	
B 11.7914		*B* 5.8913	
C 7.9584		*C* 4.6729	
μ[c] 4.42		μ[c] 4.81	
Tot. energy: −175.786521		Tot. energy: −498.378391	
bonding energy:[d] 106.0		bonding energy:[d] 144.2	
freq[e]	IR int[e]	freq	IR int
3613 ν_1(N−H str.)	33.7	3578 ν_1(N−H str.)	40.6
1630 ν_2(NCO as. str.)	500.1	1552 ν_2(NCS as. str.)	435.3
1293 ν_3(NCO s. str.)	61.8	1180 ν_3(NH in-plane def.)	47.4
1136 ν_4(NH in-plane def.)	123.8	782 ν_4(NCS s. str.)	125.9
727 ν_5(ring in-plane vib.)	4.9	616 ν_8(NH out-of-plane def.)	79.1
674 ν_8(NH out-of-plane def.)	46.0	585 ν_5(ring in-plane vib.)	17.7
584 ν_6(ring in-plane vib.)	125.6	502 ν_6(ring in-plane vib.)	101.1
409 ν_7(ring in-plane vib.)	25.8	406 ν_7(ring in-plane vib.)	14.2
236 ν_9(ring out-of-plane def.)	94.2	196 ν_9(ring out-of-plane def.)	55.8

[a] Calculated at the QCISD/6-311++G** level of theory. [b] Isotopes: H-1, N-14, C-12, O-16, S-32, Li-7. [c] Population analysis was done using the QCISD density. [d] Difference between the total energy of the complex and the sum of the energies of fragments. [e] Calculated at the B3LYP/6-311++G** level of theory (for geometry see note 35).

of the interaction. Calculations show that the two most attractive parts of the molecule are the nitrogen imine type lone pair (π_{nb}(a′)) and oxygen terminal lone pair (n_O(a′)) regions. The interaction is repulsive around the hydrogen atom, and the character of the interaction gradually changes between the most attractive and repulsive centers. This also shows that the attraction of the in-plane (a′) and out-of-plane (a″) π orbital region is different compared to each other: the in-plane nonbonding π (π_{nb}(a′)) MO region, due to the imine type lone pair character of the corresponding MO, must be more attractive than the out-of-plane π (π_{nb}(a″)) MO region. Experimental results clearly show this: both the slope parameter and peak shift are much larger for π_{nb}(a′) than for π_{nb}(a″). There is an average attractive interaction in the bonding π (π_b(a′ + a″)) MO region (slope parameter: −0.23), but the peak shift for π_b bands is smaller than that of π_{nb}, which indicates that the average well on the interaction potential is smaller. The localization of bonding and nonbonding π MOs is different, because π_{nb} MOs have a nodal surface perpendicular to the molecular symmetry plane at the carbon atom, thus π_{nb} MOs are localized on the N and O atoms, but π_b MOs have the highest electron density around the central C atom. This indicates that the interaction is more attractive at the two ends of the NCO frame than at the central carbon atom, which is in good agreement with the calculated interaction potential curves (see Figure 6). These latter show that the interaction is most attractive (deep well on the curves) around the oxygen atom and nitrogen imine type lone pair and the attractive interaction gradually decreases as the Li−C−O angle gets close to 90°. The largest negative collision energy dependence of the partial ionization cross section is observed on the oxygen terminal lone pair band, n_O(a′), in good agreement with calculations indicating a deep well on the interaction potential. In the case of such a localized band as n_O(a′) and strongly attractive interaction, a large negative peak shift of the corresponding band is expected. The observed peak shift of −20 meV, however, is very small. We do not know any explanation for this inconsistency between peak shift and collision energy dependence (slope parameter) or calculations,

but it must be noted that this is very unusual. We also note that for the methyl-substituted derivative, CH_3NCO, the $n_O(a')$ peak shift is -160 meV, which is in agreement with the attractive interaction for that molecule.[11] In general, there is good agreement with the experimental data and theoretical calculations, except the peak shift of $n_O(a')$ band.

2D-PIES investigation (see CEDPICS curves in Figure 5, slope parameters and peak shifts in Table 1) shows that the interaction between HNCS and He*(2^3S) is attractive in the π and terminal sulfur lone pair region. The attractive interaction is in agreement with calculations in the π region but not at the sulfur lone pair (see Figure 7). Calculations indicate that the interaction is attractive if the metastable atom approaches the π orbital region, but there is no deep well on the interaction potential, except the nitrogen imine type lone pair region. This latter is thus responsible for the negative peak shifts and it is the most attractive part of the molecule. Calculations show that the interaction potential is repulsive around the hydrogen atom and also in the terminal sulfur lone pair region. The large negative collision energy dependence of the ionization of $n_S(a')$ MO shows just the opposite, which is not in agreement with either calculations or previous CEDPICS investigations of the methyl-substituted derivative, CH_3NCS.[11] In the work on CH_3-NCS, practically no collision energy dependence of the ionization cross section on $n_S(a')$ band has been observed ($m = +0.014$), and since the methyl group is expected to increase electron density on the terminal sulfur lone pair, the $n_S(a')$ lone pair region in HNCS is expected be more repulsive than it is in CH_3NCS. Since we could not find any explanation for the inconsistency between calculated and experimental results, as well as between the different interactions in the sulfur lone pair region of HNCS and CH_3NCS, we thought that it might happen that the simple description of ionization as removing an electron from a MO is not valid for HNCS, thus the collision energy dependence of the $n_S(a')$ lone pair PIES band does not reflect the interaction potential in the sulfur lone pair region alone. Fortunately, the ionization of HNCS has been calculated previously by the so-called extended 2ph-TDA Green's function method,[29] which systematically takes into account the 2h1p states and the coupling of the 2h1p excitations and the simple hole states. This method predicts the breakdown of the molecular orbital model for ionization of HNCS (see Table 1). It may happen in this case that a given UPS or PIES band borrows intensity not only from a single simple transition (electron ejection from a given MO), but from several simple transitions. In such a case, the Green's function is strongly nondiagonal in the corresponding MO indices and interference effects in the cross section may be observable. Table 1 lists calculated pole strengths for ionic states, and this shows that there is remarkable nondiagonality in some orbitals such as 11a′, 2a′, and 10a′ for which the largest pole strength is unusually small as 0.5−0.7. Our interpretation for nondiagonality is that the PIES band not only originates from several MOs, but reflects the interaction potential in the related MO regions. Obviously the interpretation of the anisotropy of the interaction potential based on the localization of MOs and the one particle picture of ionization is meaningless for such a situation. We cannot say more, based on the collision energy dependence of the intensity of n_S and π_b PIES bands, that the average character of the interaction between HNCS and He*(2^3S) is attractive in the $n_S + \pi_b$ MO region. The situation is further complicated with this molecule, because calculations show other small nondiagonalities between low lying a′ MOs, too (see Table 1). There is a large negative collision energy dependence of the intensity of band 6 (see Table 1). Negative CEDPICS due to shake-up process has been observed previously for thiophene and pyrrole,[8] which also suggests the assignment of band 6 to a shake-up ionization process. We note that calculations predict the validity of the simple MO picture for the ionization of the nonbonding π_{nb} MOs of HNCS, thus the attractivity of the interaction in these MO regions can be deduced from the experiment. We also note that the breakdown of the MO picture for ionization is usually not serious for small molecules such as HNCO consisting of first-row atoms.

C. HNCOLi and HNCSLi Radicals. If the interaction is attractive between a molecule and a He*(2^3S) atom and there is large negative peak shift of the corresponding PIES band, the existence of thermodynamically stable MLi radicals is expected on the basis of the similarity between the M-He*(2^3S) and M-Li(2^2S) interaction potentials. Since the geometry of M is frozen in the Penning ionization process due to the fast relative speed of metastable atom, the peak shift is a good estimation of the bonding energy of the radical if there is no large geometry relaxation of M during the formation of M-Li, and the corresponding MO is localized. In any other case the bonding energy of the M-Li complex must be larger than the peak shift, thus the peak shift provides the estimation of the lower limit of the stabilization of M-Li. Since attractive interaction with He*(2^3S) in 2D-PIES and large negative peak shifts in PIES spectra are observed for HNCO and HNCS, the existence of thermodynamically stable HNCXLi (X = O, S) complexes is expected. To obtain information about the structure and stability of HNCOLi and HNCSLi complexes, full geometry optimizations have been performed at the QCISD/6-311++G** level. Calculated results are shown in Figure 8 and Table 2. According to calculations, HNCOLi and HNCSLi have a four-membered ring structure, similar to that of isovalence-electronic HCNOLi and HNNNLi,[1] and they can be characterized as π complexes. Total atomic charges for HNCXLi are also shown in Figure 8. According to this, there is a large positive charge on Li, close to +1, and the MO analysis indicates that this is due to the delocalization of the Li unpaired electron on the HNCX frame. The study of the formation of MOs of HNCXLi from MOs of HNCX and Li fragments (not shown) indicates that the bending of the NCX frame makes a strong LUMO(HNCX)−LUMO(Li) interaction possible, and the large stabilization of the LUMO of HNCX, as well as the delocalization of the Li 2s electron into this lower lying empty orbital, is responsible for the large bonding energy of the complex (106.0 and 144.2 kJ/mol, see Table 1) and for the positive charge on Li. We note that the same stabilizing effect has been observed for HNNNLi and HCNOLi in our previous work (see illustration of the frontier orbital interactions there).[1] The bonding energy of HNCOLi and HNCSLi is large enough to predict that these complexes would be stable at room temperature. In isolated conditions, e.g., dilute gas phase or inert solid matrix, they expected to be stable, and to assist in future identification calculated rotational constants, dipole moments, IR frequencies, and IR intensities are listed in Table 2. Potential energy surface scans at the B3LYP/6-311++G** level showed that HNCXLi complexes could form from HNCX and Li without any kinetic barrier, thus reacting Li atoms and HNCX molecules in the gas phase would provide a route for the generation of these complexes. This method has been used recently, e.g., for the generation of CH_3CNLi from CH_3CN and Li vapors.[15] We note that other two minima corresponding to the classical-type open chain HNCOLi complexes have also been found by the calculations (see note 33), but these have been shown by the B3LYP surface scan to be

only small local minima on the route of formation of the π complex. According to the calculations, the only existing isomer of HNCXLi is the four-membered ring π complex.

Calculations in this work on HNCOLi and HNCSLi and previous work on HCNOLi and HNNNLi[1] have shown that pseudohalo acids prefer to form π complexes with lithium atom. Surprisingly the classical type complex with pseudohalide terminal lone pair coordination to the metal does not exist (the kinetic barrier to isomerization is too small). An interesting point of the electronic structure is that the lithium unpaired electron is delocalized on the pseudohalide frame, and thus there is a nearly +1 total atomic charge on Li atom. This is not the case for classical type complexes (see note 33 and ref 1), where the Li valence electron stays on Li and the charge on Li is close to zero. The delocalization of the lithium 2s electron in π complexes is very interesting for cluster chemistry, where there is much interest recently to study the development of solvation from small complexes to the bulk phase.[34] One of the most interesting questions in alkali atom interaction with polar solvent is the delocalization of metal atom valence electron as more and more polar molecules are bound to the atom. Our investigations on pseudohalo acids indicate that the π system of solvent molecule can play a crucial role in this process, and studies of unsaturated solvents may provide interesting new results in this field.

VI. Conclusion

HNCO and HNCS are studied in the gas phase by Penning and He I photoelectron spectroscopies, and some information about the interaction potential between molecules (M) and He*(2^3S) atoms is deduced. Anomalies in spectroscopic data indicate the breakdown of the molecular orbital model for ionization of HNCS in the 15−20 eV region, thus information on the interaction potential between HNCS and He*(2^3S) is limited. Due to the similarity between the M-He*(2^3S) and M-Li(2^2S) interaction, fine details of the interaction potential are obtained indirectly from ab initio calculations on the computationally feasible M-Li(2^2S) system. On the basis of experimental results and calculations, the interaction between the investigated molecules and He*(2^3S) is attractive in the π orbital region of molecules, having the most attractive part at the imine type nitrogen lone pair and in the terminal oxygen lone electron pair region of HNCO. The interaction is repulsive around the hydrogen atom and in the terminal sulfur lone electron pair region of HNCS. The character of the interaction gradually changes between the attractive and repulsive centers.

Experimental investigations predict the existence of thermodynamically stable HNCOLi and HNCSLi radicals, and these radicals are characterized by ab initio calculations at the QCISD level. According to the calculations, HNCOLi and HNCSLi have a four-membered ring structure, where the lithium unpaired electron delocalize on the HNCO and HNCS frame. This latter explains the large positive charge on Li atom and large bonding energy of complexes.

Acknowledgment. We thank the Japanese Ministry of Education, Science, and Culture for a Grant in Aid for Scientific Research in support of this work. T.P. thanks the Japan Society for the Promotion of Science (JSPS) for a JSPS Invitation Fellowship (IDNo. L98519) and the Hungarian Scientific Research Found (OTKA Grant F022031) in support of this work.

References and Notes

(1) Pasinszki, T.; Kishimoto, N.; Ohno, K. *J. Phys. Chem. A* **1999**, *103*, 6746.

(2) Ohno, K.; Yamakado, H.; Ogawa, T.; Yamata, T. *J. Chem. Phys.* **1996**, *105*, 7536.

(3) Pasinszki, T.; Yamakado, H.; Ohno, K. *J. Phys. Chem.* **1995**, *99*, 14678.

(4) Takami, T.; Mitsuke, K.; Ohno, K. *J. Chem. Phys.* **1991**, *95*, 918.

(5) Takami, T.; Ohno, K. *J. Chem. Phys.* **1992**, *96*, 6523.

(6) Ohno, K.; Okamura, K.; Yamakado, H.; Hoshino, S.; Takami, T.; Yamauchi, M. *J. Phys. Chem.* **1995**, *99*, 14247.

(7) Yamakado, H.; Yamauchi, M.; Hoshino, S.; Ohno, K. *J. Phys. Chem.* **1995**, *99*, 17093.

(8) Kishimoto, N.; Yamakado, H.; Ohno, K. *J. Phys. Chem.* **1996**, *100*, 8204.

(9) Yamauchi, M.; Yamakado, H.; Ohno, K. *J. Phys. Chem. A* **1997**, *101*, 6184.

(10) Yamakado, H.; Ogawa, T.; Ohno, K. *J. Phys. Chem. A* **1997**, *101*, 3887.

(11) Pasinszki, T.; Yamakado, H.; Ohno, K. *J. Phys. Chem.* **1993**, *97*, 12718.

(12) Ohno, K.; Kishimoto, N.; Yamakado, H. *J. Phys. Chem.* **1995**, *99*, 9687.

(13) Kishimoto, N.; Yokoi, R.; Yamakado, H.; Ohno, K. *J. Phys. Chem. A* **1997**, *101*, 3284.

(14) Kishimoto, N.; Aizawa, J.; Yamakado, H.; Ohno, K. *J. Phys. Chem. A* **1997**, *101*, 5038.

(15) Ohshimo, K.; Tsunoyama, H.; Yamakita, Y.; Misaizu, F.; Ohno, K. *Chem. Phys. Lett.* **1999**, *301*, 356.

(16) Eland, J. H. D. *Philos. Trans. R. London A* **1970**, *268*, 87.

(17) Cradock, S.; Ebsworth, E. A. V.; Murdoch, J. D. *J. Chem. Soc., Faraday Trans. 2* **1972**, *68*, 86.

(18) Gunther, P.; Meyer, R. *Z. Elektrochem.* **1935**, *41*, 541.

(19) Mitsuke, K.; Takami, T.; Ohno, K. *J. Chem. Phys.* **1989**, *91*, 1618.

(20) Gardner, J. L.; Samson, J. A. R. *J. Electron. Spectrosc. Relat. Phenom.* **1976**, *8*, 469.

(21) Kimura, K.; Katsumata, S.; Achiba, Y.; Yamazaki, T.; Iwata, S. *Handbook of He I Photoelectron Spectra of Fundamental Organic Molecules*; Japan Scientific Press: Tokyo, 1981.

(22) (a) Rothe, E. W.; Neynaber, R. H.; Trajillo, S. M. *J. Chem. Phys.* **1965**, *42*, 3310. (b) Niehaus, A. *Adv. Chem. Phys.* **1981**, *45*, 399. (c) Hotop, H. *Radiat. Res.* **1974**, *59*, 379. (d) Haberland, H.; Lee, Y. T.; Siska, P. E. *Adv. Chem. Phys.* **1981**, *45*, 487.

(23) Yamada, K. *J. Mol. Spectrosc.* **1980**, *79*, 323.

(24) Yamada, K.; Winnewisser, M.; Winnewisser, G.; Szalanski, L. B.; Gerry, M. C. L. *J. Mol. Spectrosc.* **1980**, *79*, 295.

(25) Boys, S. F.; Bernardi, F. *Mol. Phys.* **1970**, *10*, 553.

(26) *Gaussian 94*, Revision C.3; Frisch, M. J.; Trucks, G. W.; Schlegel, H. B.; Gill, P. M. W.; Johnson, B. G.; Robb, M. A.; Cheeseman, J. R.; Keith, T.; Petersson, G. A.; Montgomery, J. A.; Raghavachari, K.; Al-Laham, M. A.; Zakrzewski, V. G.; Ortiz, J. V.; Foresman, J. B.; Cioslowski, J.; Stefanov, B. B.; Nanayakkara, A.; Challacombe, M.; Peng, C. Y.; Ayala, P. Y.; Chen, W.; Wong, M. W.; Andres, J. L.; Replogle, E. S.; Gomperts, R.; Martin, R. L.; Fox, D. J.; Binkley, J. S.; Defrees, D. J.; Baker, J.; Stewart, J. P.; Head-Gordon, M.; Gonzalez, C.; Pople, J. A. Gaussian, Inc.: Pittsburgh, PA, 1995.

(27) von Niessen, W.; Schirmer, J.; Cederbaum, L. S. *Comput. Phys. Rep.* **1984**, *1*, 57. Cederbaum, L. S.; Domcke, W. *Adv. Chem. Phys.* **1977**, *36*, 205.

(28) Zeiss, G. D.; Chong, D. P. *J. Electron. Spectrosc. Relat. Phenom.* **1980**, *18*, 279.

(29) von Niessen, W.; Cederbaum, L. S.; Schirmer, J.; Diercksen, G. H. F.; Kraemer, W. P. *J. Electron. Spectrosc. Relat. Phenom.* **1982**, *28*, 45.

(30) Hotop, H.; Niehaus, A. *Z. Phys.* **1969**, *228*, 68.

(31) Ohno, K.; Mutoh, H.; Harada, Y. *J. Am. Chem. Soc.* **1983**, *105*, 4555.

(32) Ohno, K.; Harada, Y. Penning Ionization − The Outher Shape of Molecules. In *Theoretical Models of Chemical Bonding Part 3*; Maksič, Z. B., Ed.; Springer-Verlag: Berlin, 1991.

(33) Open chain HNCOLi complexes (QCISD(fc)/6-311++G**). (a) Li coordinated to the oxygen terminal lone pair: N−H = 1.006 Å, N−C = 1.204 Å, C−O = 1.179 Å, O−Li = 1.979 Å, HNC = 128.7°, NCO = 171.5°, COLi = 146.9°; total energy: −175.753003 au; total atomic charge on Li: +0.02. (b) Li coordinated to the nitrogen imine type lone pair: N−H = 1.015 Å, N−C = 1.241 Å, C−O = 1.156 Å, N−Li = 2.104 Å, HNC = 116.9°, NCO = 172.7°, LiNC = 124.3°; total energy: −175.755994 au; charge on Li: +0.01.

(34) Schulz, C. P.; Hertel, I. V. Solvated Atoms in Polar Solvents. In *Clusters of Atoms and Molecules II*; Haberland, H., Ed.; Springer-Verlag: Berlin-Heidelberg, 1994; pp 7−18.

(35) Geometry of HNCO-π at the B3LYP/6-311++G** level: N−H = 1.010 Å, N−C = 1.308 Å, C−O = 1.246 Å, N−Li = 1.881 Å, O−Li = 1.902 Å, HNC = 115.3°, NCO = 126.2°; total energy: −176.272881 au.